

Rigor-like Structures from Muscle Myosins Reveal Key Mechanical Elements in the Transduction Pathways of This Allosteric Motor

Yuting Yang,^{1,5,6} S. Gourinath,^{1,2,5} Mihály Kovács,³ László Nyitrai,³ Robbie Reutzler,¹ Daniel M. Himmel,⁴ Elizabeth O'Neill-Hennessey,¹ Ludmilla Reshetnikova,¹ Andrew G. Szent-Györgyi,^{1,*} Jerry H. Brown,¹ and Carolyn Cohen^{1,*}

¹Rosenstiel Basic Medical Sciences Research Center, Brandeis University, Waltham, MA 02454, USA

²School of Life Sciences, Jawaharlal Nehru University, New Delhi 110067, India

³Department of Biochemistry, Eötvös Loránd University, H-117 Budapest, Pázmány P. Sétány 1/C, Hungary

⁴Center for Advanced Biotechnology and Medicine and Department of Chemistry and Chemical Biology, Rutgers University, Piscataway, NJ 08854, USA

⁵These authors contributed equally to this work.

⁶Present address: Department of Biological Chemistry, University of Michigan Medical School, Ann Arbor, MI 48109, USA.

*Correspondence: ccohen@brandeis.edu (C.C.), szentgyorgyi@brandeis.edu (A.G.S.-G.)

DOI 10.1016/j.str.2007.03.010

SUMMARY

Unlike processive cellular motors such as myosin V, whose structure has recently been determined in a “rigor-like” conformation, myosin II from contracting muscle filaments necessarily spends most of its time detached from actin. By using squid and sea scallop sources, however, we have now obtained similar rigor-like atomic structures for muscle myosin heads (S1). The significance of the hallmark closed actin-binding cleft in these crystal structures is supported here by actin/S1-binding studies. These structures reveal how different duty ratios, and hence cellular functions, of the myosin isoforms may be accounted for, in part, on the basis of detailed differences in interdomain contacts. Moreover, the rigor-like position of switch II turns out to be unique for myosin V. The overall arrangements of subdomains in the motor are relatively conserved in each of the known contractile states, and we explore qualitatively the energetics of these states.

INTRODUCTION

The recent determination of the atomic structure of the nucleotide-free state of the specialized nonmuscle myosin V motor is the first picture we have of a conformation identified as a strong, actin-bound “rigor-like” state (Coureux et al., 2003, 2004). Paradoxically, this structure was obtained in the absence of actin. The head (subfragment 1 or S1) of muscle as well as nonmuscle myosins consists of an ATP-driven motor domain as well as a lever arm that amplifies small conformational changes in the motor. Previously, three weak actin-binding states of the head in a number of muscle myosins (myosin II) have been char-

acterized at atomic resolution: the post-rigor state (previously called “near-rigor” [Rayment et al., 1993b]); the pre-power stroke or transition state (Dominguez et al., 1998; Fisher et al., 1995; Gourinath et al., 2003; Houdusse et al., 2000), and the “internally uncoupled” state (previously called “detached”) (Houdusse et al., 1999; Himmel et al., 2002). The nature of the bound nucleotide and crystallization conditions determines which state the structure adopts. (Some of the post-rigor structures could also be obtained in the absence of nucleotide, but had a sulfate, instead, in the nucleotide-binding pocket.) Moreover, these structural studies showed that the motor of the myosin head can be pictured as consisting of four major subdomains, which are linked by highly conserved, flexible, single-stranded joints, including switch II, the “relay,” the so-called “SH1” helix, and the less flexible “strut” (Houdusse et al., 1999; Fujita-Becker et al., 2006) (see Figure 1). One of these four subdomains, the so-called “converter” (Houdusse and Cohen, 1996), is directly linked to the light-chain domain, now commonly called the “lever arm,” and controls its orientation in the various states of the actomyosin cycle. The structures of these weak binding states have revealed many of the mechanical elements in the head that are related to the transduction pathway from the nucleotide-binding site to the converter/lever arm movement, which is essential for the power stroke.

The most striking feature of the rigor-like conformation of the nonmuscle myosin V motor is the closure of the major cleft in the 50 kDa subdomain near the actin interface (predicted by Rayment and colleagues as early as 1993) (Rayment et al., 1993a). This conformation fits without distortion into the density seen by electron microscopic reconstructions of myosin II-decorated actin (Holmes et al., 2004). By contrast, this cleft is relatively open in the weak actin-bound states. This singular structure thus discloses major aspects of the transduction pathway between actin binding, the power stroke, and product release. The “transducer,” a key ensemble of mechanical elements in this pathway, has been identified as the β sheet region

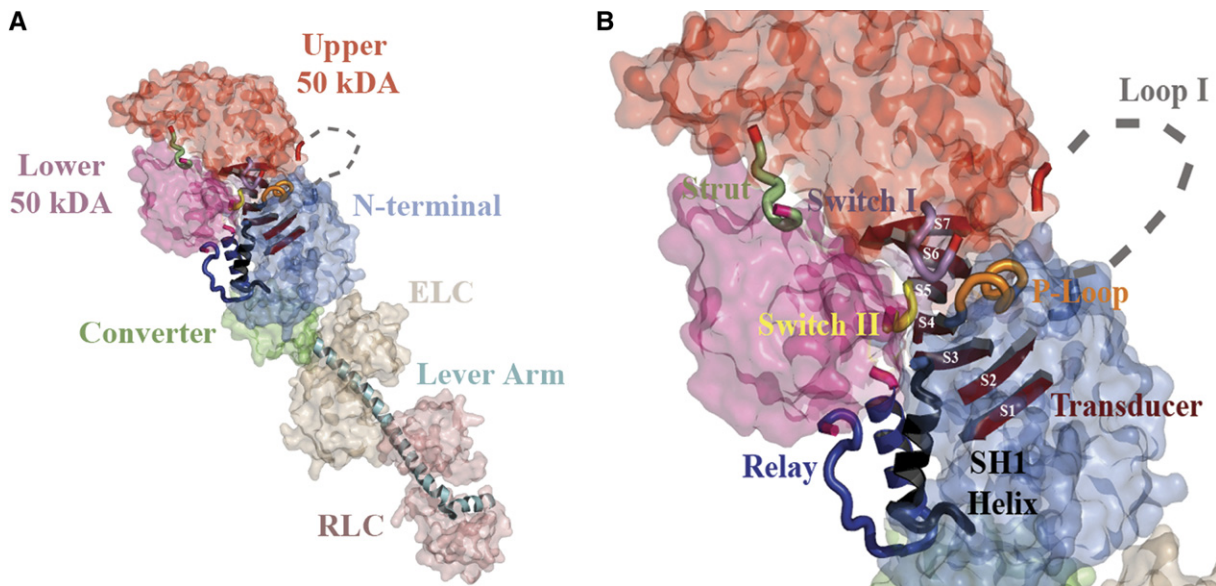


Figure 1. Structure of a Rigor-like Muscle Myosin S1

(A and B) Displayed is the nucleotide-free myosin head (S1) from the funnel retractor muscle of *Loligo* (squid) in the rigor-like conformation. The subdomains are depicted by space-filling models. Key loops (such as switch I, the P loop, and the relay) and connections between the subdomains (such as the strut, switch II, the SH1 helix, and the transducer's loop 1 and β sheet) are illustrated in ribbon/cartoon form. (A) Overall structure. (B) Magnified view of the motor domain.

with associated loops (such as switch I) (Coureux et al., 2004). The insights provided by both the weak and strong actin-binding structures are now beginning to clarify the allosteric transitions in this complex molecular machine.

Here, we report rigor-like conformations in muscle myosins at atomic resolution. These structures were visualized by using crystals of nucleotide-free S1 from a number of molluscan muscles (myosin II). (These include the fast funnel retractor muscle of squid and fast striated and relatively slow “catch” muscles of the sea scallop.) Despite the diverse kinetic/functional properties of these isoforms, these structures display key rigor-like features identified in myosin V, including a switch I position away from the nucleotide pocket and a fully closed 50 kDa cleft at the actin-binding interface. A comparison of these molluscan myosin rigor-like structures with that of myosin V, as well as other previously reported nucleotide-free structures of the motor domains of *Dictyostelium discoideum* myosin II (Reubold et al., 2003) and pig myosin VI (Menetrey et al., 2005), has revealed rigor-like structural features that appear to be conserved in many classes of myosin. Taken together, these results show that the overall “counterclockwise” orientation of the 50 kDa cleft, rather than the precise extent of its closure, is most directly related to the rigor-like position of switch I. The structure of the myosin V motor was originally selected because of its specialized kinetic properties, such as high duty ratio and rapid binding to actin, suggesting that this myosin class would readily adopt the rigor-like conformation, even in the absence of actin (De La Cruz et al., 1999). Our results now show that the rigor-like conformation in the absence of actin is accessible to a greater variety of myosin classes than pre-

viously thought. We also describe here how sequence differences between isoforms at interdomain connections are present in these various structures, and how they may account for variations in the kinetic/functional properties of these motors. These results also suggest the kinds of conformational changes that might be found in yet unobserved states in which both nucleotide (ADP) and actin are strongly bound.

RESULTS AND DISCUSSION

Conserved Features of the Rigor-like/Nucleotide-free Conformations in Various Myosin Classes

We have made the surprising discovery that well-ordered crystals of the nucleotide-free/rigor-like state of the myosin motor in the absence of actin are readily obtained in widely different classes of this molecule. These results reveal that the overall structure and many of the details of myosin II S1 from *Loligo pealei* (squid) fast funnel retractor muscle (Figure 1) and from *Placopecten magellanicus* (sea scallop) slow catch and fast striated muscles are quite similar to one another and to previously reported structures of the nucleotide-free motor domains of myosin V, *Dictyostelium* myosin II, and myosin VI (see Table 1).

Analysis of these findings indicates that there appear to be a number of conserved rigor-like features in all of these actin-free, nucleotide-free structures. This in vitro state in the current structures was produced by starting with actin-free S1, in the presence of 0.2–0.5 mM MgADP (used to stabilize the protein during its purification); the nucleotide was then removed by dialysis before crystallization (see Experimental Procedures) to obtain the rigor-like

Table 1. The Orientation of Myosin's 50 kDa Cleft in the Rigor-like State Is Highly Conserved

Isoform (with PDB ID; CAPS, from Current Study)	Cleft Orientation: Angle (°) between C α s of N-Terminal Subdomain Residues 145, 185, and		Cleft Closure: Distance (Å), at Indicated Locations of the Cleft, between C α s of the Indicated Upper and Lower 50 kDa Residues			
	Upper 50 kDa Subdomain Residue 424	Lower 50 kDa Subdomain Residue 601	Far Outer Cleft (Near Actin) 373–543	Outer Cleft (Strut) 424–601	Inner Cleft 281–474	Far Inner Cleft (Switches) 241–470
Rigor-like						
Squid (2OVK)	127	117	13.2	7.8	9.8	7.3
Myosin V (1oe9)	129	120	13.2	7.2	9.6	7.9
Myosin VI (2bkh)	129	118	18.2	8.3	11.1	10.3
<i>Placo</i> catch (2OS8)	126 ^a	115 ^a	14.3	8.4	12.9	10.4
<i>Dicty</i> (2aka)	129	115	20.3	10.4	11.0	7.8
Post-Rigor						
Squid (2OY6)	150	129	20.1	14.4	16.1	13.4
<i>Argo</i> striated (1sr6)	147	128	20.1	13.1	16.3	14.1
Myosin V (1w7j)	155/149 ^a	133/127 ^a	20.7	14.2	16.2	12.9
<i>Placo</i> catch (2OTG)	147	128	20.9	13.3	16.5	13.8
<i>Dicty</i> (1mmd)	149	128	22.2	14.4	15.3	12.4
Chicken striated (2mys)	148	126	23.0	14.5	16.8	14.8
Pre-Power Stroke						
<i>Argo</i> striated (1qvi)	155	134	25.4	13.9	12.5	8.8
<i>Dicty</i> (1vom)	154	133	22.5	13.4	12.6	8.9
Chicken smooth (1br1)	154	134	22.9	13.3	11.8	8.8

The orientation of myosin's 50 kDa cleft, but not the extent of its closure, is highly conserved in the various nucleotide-free structures (including *Dictyostelium* and myosin VI). Also see Figure 3. This "rigor-like" organization of the subdomains is distinctive from that in the other states. Squid numbering is used. Italicized and bold-face text indicate isoform(s) with the most open and closed clefts, respectively, among the nucleotide-free/rigor-like structures. "*Placo*" indicates sea scallop, and "*Argo*" indicates bay scallop. Residue ranges for structural features in squid myosin S1 are as follows: upper 50 kDa subdomain, 217–452 and 607–625; lower 50 kDa subdomain, 643–666 and 466–598; converter, 708–778; N-terminal subdomain, 86–165; SH3 motif, 1–85; P loop, 175–183; switch I, 237–247; switch II, 463–474; strut, 601–606; SH1 helix, 695–708; relay loop, 493–520; relay helix, 474–507; loop 1, 197–219.

^a See the legend in Supplemental Data.

structures (Figure 2A). In the absence of nucleotide, switch I is not positioned above the P loop, but is instead close to switch II (see below and Figure 2B). The repositioning of switch I and its subsequent interactions then lead to distinctive counterclockwise positions of the upper and lower 50 kDa subdomains (relative to the N-terminal subdomain, as viewed in Figures 1, 2A, and 3; see also Table 1). These subdomain positions result in a relatively closed 50 kDa cleft (albeit to a lesser degree in *Dictyostelium* and myosin VI, see below) (see also Table 1), a "fully twisted" seven-stranded β sheet (consisting of both parallel and antiparallel strands) spanning the upper 50 kDa and N-terminal subdomains (Figure 4), and a number of specific interactions between the subdomains; these features are different from those of the pre-power stroke and post-rigor conformations. (The term "beta" will henceforth be omitted in referring to one of the strands in the β sheet.) The rigor-like/nucleotide-free structures also share a straight relay helix and nearly identical "down" positions for the converter (myosin VI excepted), close to that seen in the

post-rigor structures (Figure 5). It appears that diverse myosins with different kinetic and functional properties can have similar rigor-like conformations in the absence of actin. Note that the small differences in their conformations discussed below probably cannot be detected at the resolution afforded by electron microscopy (see Holmes et al., 2004).

Isoform-Specific Differences in the Rigor-like State

These current myosin II structures allow us to distinguish between certain conformational features that characterize most myosins in the rigor-like state and other isoform-specific differences that are due to sequence variations. For comparative purposes, we use the corresponding post-rigor structures (when available), since this state appears to follow the rigor-like state directly in the contractile cycle.

The Active Site

Conformations in the weak actin-binding structures are related to the content of the nucleotide-binding pocket,

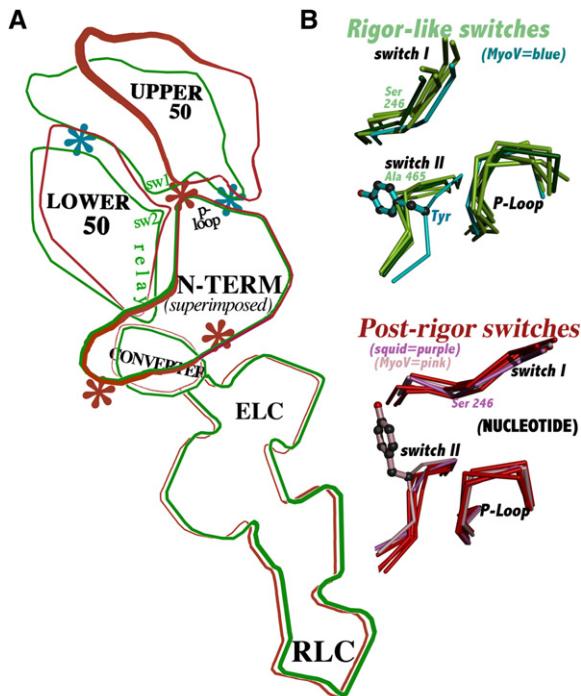


Figure 2. Comparison of the Rigor-like and Post-Rigor States of Muscle Myosin S1 and Its Active Site

(A and B) Detailed legends for all figures are supplied in [Supplemental Data](#). (A) Schematic overlay of (squid) S1 in the two states (see text). The rigor-like state is shown in green, and the post-rigor state is shown in red. Thicker lines indicate proximity to the reader. The overall conformational differences between these (and the pre-power stroke) states are generally conserved in the different isoforms. The locations of interdomain interactions that nevertheless appear to preferentially stabilize the high-duty ratio non-muscle myosin V in a rigor-like conformation and some of the low-duty ratio myosin II isoforms in a non-rigor-like (actin-detached) conformation are indicated here with blue and red asterisks, respectively (also see text and [Figures 3–5](#)). (B) The rigor-like location of switch II in the various myosin II and VI structures (green), which have small side chains at (squid) position 465, differs from that in myosin V (blue), in which 465 is a tyrosine. The locations of both switch I and switch II away from the nucleotide and near each other force the tyrosine to adopt a “g⁻” rotamer. The myosin V switch II is displaced toward the P loop of the N-terminal subdomain in the rigor-like state to avoid a clash of this rotamer with helix W (not shown). In the post-rigor state (red), switch I (including Ser246) is near the nucleotide and relatively far from switch II. Here, the tyrosine has room to adopt the “g⁺” rotamer and does not perturb the arrangement of the active site elements.

which is “sensed” by switches I and II. Correspondingly, a key feature that distinguishes myosin’s rigor-like active site from its post-rigor active site is the location of switch I near, and directly “above,” switch II (as seen in [Figure 2B](#)). This close relationship between the switches in the rigor-like state appears to be conserved for the myosin II structures that we are reporting and for all other myosin structures currently available. Myosin V, however, displays a distinctive feature: an additional small (~ 1.5 Å) repositioning of the main chain of switch II, in the perpendicular direction, allows two additional H bonds to be made

with the P loop at the end of strand 4. Note that the close association of strand 4 and switch II in myosin V was originally interpreted as being a “hallmark” of the rigor-like state in all myosins ([Coueux et al., 2004](#)).

This unusual close association of switch II with strand 4 in the myosin V rigor-like state appears, however, to be a steric consequence of the large tyrosine residue in myosin V at switch II, position 465 (squid numbering used throughout, unless otherwise noted; thus, squid 465 = myosin V 439). The avoidance of atomic collisions of its side chain with neighboring elements (switch I and helix W) in the rigor-like state appears to cause the displacement of switch II toward strand 4. By contrast, in myosin II and myosin VI, this residue is small (Ala or Ser), and there is no steric effect on switch II (see [Figure 2B](#) and legend for details).

The post-rigor structures of these myosins can be used as a kind of “control” to test the notion of steric hindrance by the tyrosine. The close association of switch II with strand 4 that is found in the rigor-like state of myosin V does not occur in any of the post-rigor structures, including that of myosin V. Here, the two switches are relatively far apart, and the tyrosine side chain is not obstructed.

Cleft Closure

The extent of myosin cleft closure is a critical component of the transduction pathway leading to the power stroke. The positions of switches I and II in the rigor-like state are associated with counterclockwise orientations of the 50 kDa subdomains and the cleft between them about the N-terminal subdomain, relative to their orientations in the post-rigor state ([Figure 2A](#) and [Table 1](#)). The change in the position of switch I is greater than that of switch II between these two states; thus, the movement in the upper 50 kDa subdomain is greater than in the lower. (Note, also, that there is a lateral component to the repositioning of these subdomains [[Figure 2A](#), and see legend].) The coordinated repositioning of both subdomains leads to the closing of the 50 kDa cleft in the nucleotide-free structures ([Table 1](#)).

Differences in the extent and location of the cleft closure, nevertheless, do occur among the six nucleotide-free structures ([Figure 3](#); [Table 1](#)). While both the inner (i.e., nearest the nucleotide site) and the outer (nearest actin) parts of the 50 kDa cleft are “fully closed” in myosin V and squid (see [Figures 3A](#) and [3B](#)), they are only partially closed in myosin VI ([Figure 3E](#)). In the *Dictyostelium* nucleotide-free structure ([Figure 3D](#)), the outer cleft is only partially closed and the inner cleft is fully closed. The reverse occurs in the catch and striated sea scallop nucleotide-free structures ([Figure 3C](#)); here, the outer cleft is nearly as fully closed as that of myosin V or squid, and the inner cleft is only partially closed.

We can relate certain structural features to some of the specific differences in the extent of cleft closure in these different myosins. It appears that, while the extent of inner cleft closure is determined by the relative positions of the P loop, switch I, and switch II, the extent of the outer cleft closure involves variable positions of the strut. This semiflexible connection between the 50 kDa subdomains, rather near the actin interface, helps constrain their

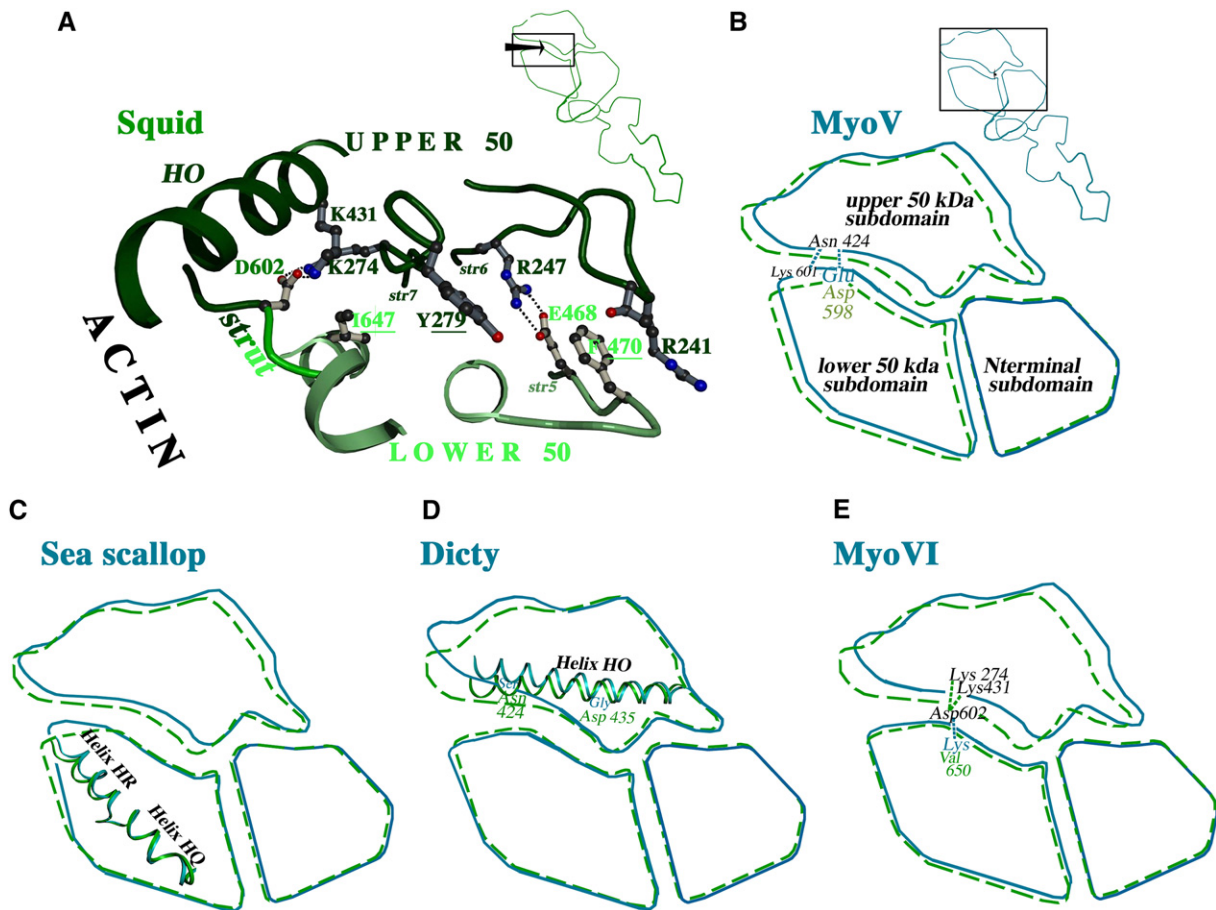


Figure 3. Conserved and Variable Features of the Rigor-like 50 kDa Cleft

(A–E) The schematic S1 inset on this and subsequent figures shows the region that is magnified (box) and the viewpoint (arrow). Squid sequence numbering is used. (A) Displayed are selected interactions between the upper (dark green) and lower (light green) 50 kDa subdomains made in the squid rigor-like structure that are also made (with identical or homologous residues) in the other isoforms studied when the corresponding part of their cleft is also fully closed. Interactions include H-bonded/electrostatic contacts (dotted lines) and extensive burial of certain apolar residues (underlined labels). (B–E) Variations in crosscleft contacts, as well as in the orientations of the upper and lower 50 kDa subdomains or of subregions within them, help determine the extent of inner and outer cleft closure in the various isoforms (the green, dashed line shows squid for comparison.) (B) Myosin V displays the most closed cleft in the strut region (also see Table 1), perhaps due to a “complex H-bond link” (blue, dotted lines) between Asn424, Lys601, and Glu598 not seen in any other isoform; position 598 is aspartate in squid and sea scallop, and 424 is serine in *Dictyostelium* (see below for myosin VI). (C) A slightly modified orientation of helix HR relative to helix HQ yields a fully closed outer but incompletely closed inner cleft in catch and striated sea scallop S1. (D) Curvature of helix HO about a *Dictyostelium*-specific glycine at 435 contributes to its fully closed inner but partially open outer cleft. (E) The entire cleft of myosin VI is incompletely closed. A myosin VI-specific lysine at position 650 appears to disrupt the interdomain 602–274–431 complex salt link made from the strut.

relative orientations (see Figure 1). It appears that the uniquely tightly closed outer cleft of myosin V (Table 1) is produced by a network of H bonds (Figure 3B), one of which is at the lower part of the outer surface of the strut. On the other side of the strut, a complex salt link of conserved residues, involving the middle of the strut and 2 residues of the upper 50 kDa subdomain, appears to be strongest when the outer part of the cleft is most closed (Figure 3A), partially broken in those nucleotide-free structures (e.g., *Dictyostelium*) in which this region of the cleft is more open, and relatively strong again in many of the post-rigor structures. It is possible that this complex salt link undergoes a breaking-reforming process in the transition from the rigor-like state to the post-rigor state. In contrast,

the H-bond network seen in the myosin V rigor-like structure is necessarily disrupted in the post-rigor state, in which the outer cleft in all isoforms is more open than in the rigor-like state. These observations suggest that the making and breaking of certain key linkages involving the strut play a critical role in the extent of outer cleft closure. Similar interactions are involved in determining the degree of closure in the inner region of the cleft. These crosscleft linkages (see Figure 3A), even those involving conserved residues, are stretched or completely broken when the corresponding part of the cleft is incompletely closed.

These comparative studies on the cleft are a starting point for correlating the degree of closure of various

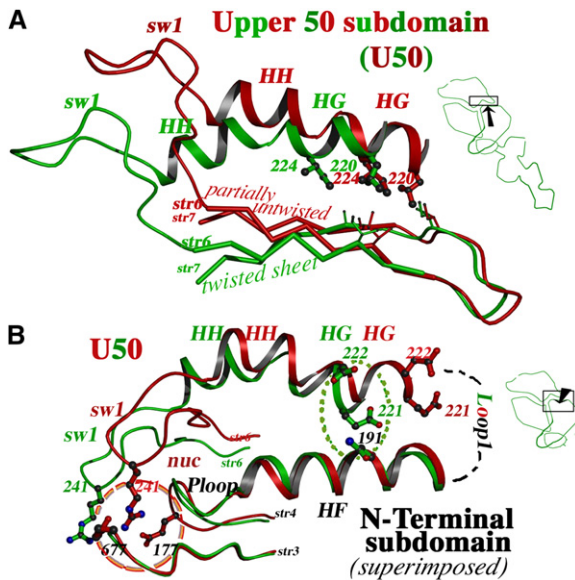


Figure 4. Conserved Promoters and Variable Inhibitors of Conformational Changes in Myosin's Transducer

(A and B) Such features are functionally important since the upper 50 kDa (colored labels) and N-terminal (black labels) subdomains, which are spanned by the transducer, are closely connected to one another in both the rigor-like (green) and post-rigor (red) states. (A) Side view (in squid S1) of the upper 50 kDa subdomain elements of the transducer. One conserved promoter of the contractile cycle is the local twisting/untwisting (rather than a register shift) between the upper 50 kDa subdomain and N-terminal subdomain sections of the central β sheet (also see [B]). Another is a repeat of similar apolar residues (Val, Ile, or Leu) at 220 and 224. These side chains nearly substitute for one another in the two states as HG shifts by nearly one helical turn relative to the β sheet (and HF, see [B]). (B) Top view of both (squid) subdomains. (Strand 5 at their boundary is not shown for clarity.) Sequence differences between isoforms may help stabilize different states. A complex salt link between Arg241, Glu677, and Glu177 (red, dashed circle) is made only in the non-rigor-like position of switch I close to the P loop, and only in certain fast striated muscle myosins. Conversely, a complex salt link between acidic side chains of HG 222/221 and HF residue 191 is possible only in the rigor-like state of myosin V and myosin VI (green, dotted circle). (See text. Also, for a description of loop 1, see text and Supplemental Data.)

regions of the cleft with particular functional aspects of these six isoforms. The significance of the closure of the outer part of the cleft is relatively straightforward: it is required for strong and productive binding to actin (Rayment et al., 1993a; Coureux et al., 2004; Geeves and Holmes, 2005). The temperature dependence of this association (which measures the rate of binding) in the absence of nucleotide reveals whether the structure of isolated S1 is truly rigor like—that is to say, whether or not additional structural changes are required for strong binding to actin (Coureux et al., 2003). At present, we have this information for some of the myosins that we are comparing. In the case of myosin V, the relatively limited data on this point appear to show a very small temperature dependence of the rate of binding to actin, and they have been interpreted as being consistent with a purely diffusion-limited reaction (Coureux et al., 2003; De La Cruz et al., 1999). Corre-

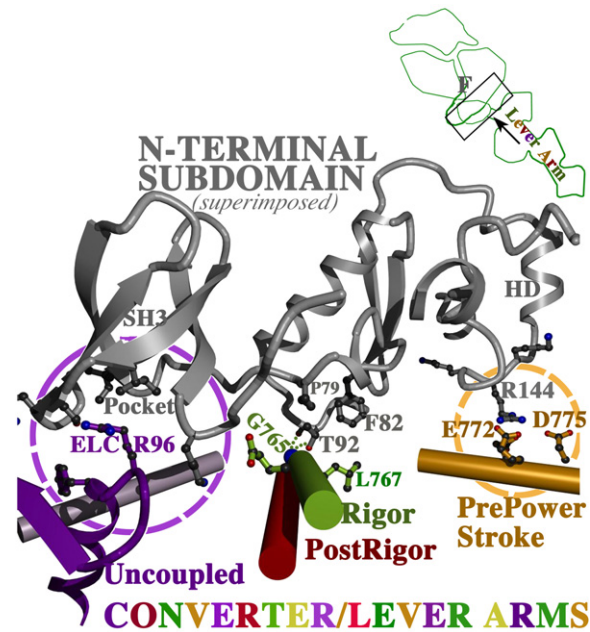


Figure 5. Four Distinct Conformational States for the Myosin II Converter/Lever Arm Module Can Now Be Discerned

Scallop S1 structures and sequence numbering are used in this figure. In the rigor-like state (green), two H bonds (dotted lines) between Thr (or Ser) 92 of the N-terminal subdomain (ribbons) and the main-chain nitrogen of Gly765 of the converter's C-terminal helix (cylinder), as well as the burial of nearby apolar residues (e.g., Pro79, Phe82, and Leu767), are well conserved in the various myosin II and V structures. These interactions are either somewhat weakened (squid, *Dictyostelium*) or totally broken (sea scallop catch [shown here] or myosin V) in the post-rigor structures (red). The converter/lever arm module is swung to other binding sites on the N-terminal subdomain in its "internally uncoupled" (purple) and pre-power stroke state (orange) positions (bay scallop striated shown). These two actin-detached states are stabilized, respectively, by SH3-pocket filling and electrostatic interactions in the myosin II structures; these interactions cannot be made in the same way in myosin V (see text). The fulcrum of the swinging converter/lever arm module (also see text) is located behind the plane of the paper, and its position is indicated by "F" in the inset.

spondingly, in this isoform, no change in the outer cleft would be predicted to take place in the presence of actin. Experiments (between 5°C and 27°C) have now been carried out on the molluscan myosins for which we have structural information (squid, sea scallop catch, and sea scallop striated S1). These data also show a small temperature dependence, which is less than in rabbit S1 (Figure 6). Moreover, the temperature dependence of complex formation with actin is essentially the same for sea scallop and murine myosin Va S1s. Taken together, it appears that these rigor-like structures, formed in the absence of nucleotide, require only the closure or near closure of the outer cleft for strong actin binding, despite differences in the degree of closure in the inner cleft. Further solution studies on the *Dictyostelium* myosin motor domain, now in progress (M.K., unpublished data), should reveal whether mechanisms, such as "induced fit," are required for its strong binding to actin.

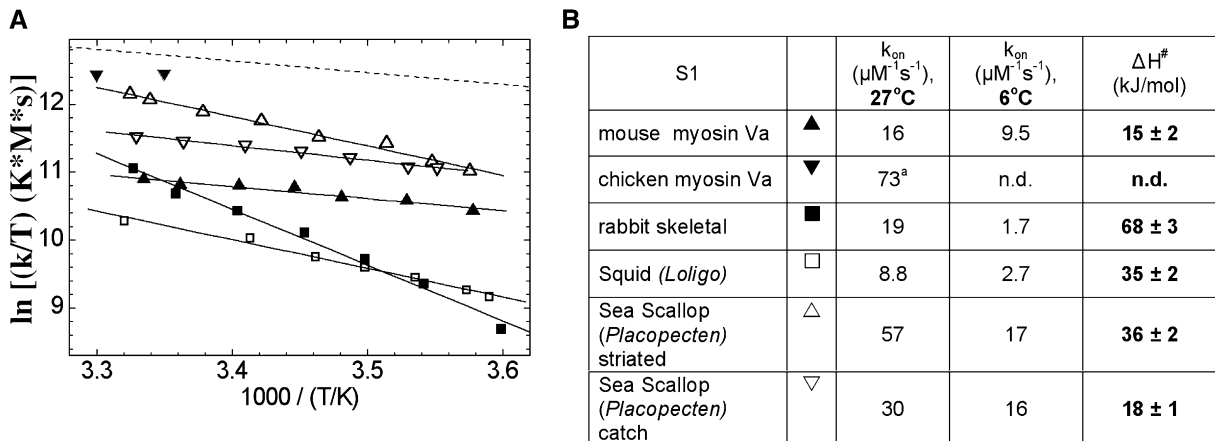


Figure 6. Temperature Dependence of S1 Binding to Actin

(A) Eyring plots of the rate constants of S1 binding to pyrene-actin. Solid squares, skeletal S1; solid, right-side up triangles, mouse myosin Va S1; solid, upside down triangles, chicken myosin Va S1 (Sweeney and Houdusse, 2004); open squares, squid S1; open, right-side up triangles, sea scallop striated S1; open, upside down triangles, sea scallop catch S1. The slope of the Eyring plot of the second-order pyrene-actin binding rate constant of molluscan S1s is close to that of mouse myosin Va S1 and to the estimated theoretical slope of a purely diffusion-limited reaction, where k is inversely proportional to the viscosity of the solution (cf. dashed line: its intercept is arbitrary) (Atkins, 1990). The slope is essentially the same for mouse myosin Va and sea scallop catch S1.

(B) Rate constants ($\mu\text{M}^{-1}\text{s}^{-1}$) and activation enthalpies of S1 binding to pyrene actin. (ΔS^\ddagger values are not presented. They are difficult to determine accurately because the use of several estimated parameters is necessary in the calculations.) n.d. = not determined. ^a = measured at 25°C (De La Cruz et al., 1999).

We will discuss later how certain differences in cleft closure, observed in these nucleotide-free structures, may be useful in modeling as yet unobserved rigor-related states (such as strong actin, strong nucleotide binding). Whatever the detailed differences in cleft closure of these structures (Table 1), however, it appears that the overall orientation of the cleft's subdomains (relative to the N-terminal subdomain or converter) (Table 1) is well conserved in all of these structures and may be considered a criterion for a rigor-like state.

Some Properties of the Transducer

The discovery of the rigor-like conformation of myosin V led to the recognition of the significance of the so-called transducer in controlling the reciprocal relation between actin binding to a closed 50 kDa cleft and product release from an open nucleotide-binding site (Coureux et al., 2003, 2004). The central mechanical element of the transducer is a seven-stranded β sheet, which connects the upper 50 kDa and N-terminal subdomains by main chain hydrogen bonds, as well as side chain interactions (Figure 4) (Coureux et al., 2004). In the rigor-like state, the full extent of right-handed twisting of the β sheet differs markedly from that in other states. As discussed in the "Energetics" section below, cleft closure sets into motion a series of mechanical events involving certain strands of the β sheet and connected switches and helices, which produce converter/lever arm motion and nucleotide release.

Special conserved features in this key mechanical region facilitate transitions between structural states in these diverse isoforms of myosin. The positions of switch I and switch II, relative to the P loop, allow a fully twisted β sheet in all of the nucleotide-free/rigor-like structures

(see Figure 4). By contrast, the β sheet is "partially untwisted" in all of the post-rigor structures (see Figure 4), "nearly untwisted" in the internally uncoupled state (see below), and "untwisted" in the pre-power stroke state (figure not shown). One role of the twisting/untwisting is that it allows for the preservation of the strand register and the H-bonding pattern (albeit with somewhat different geometries) throughout the entire β sheet in the transition between states. These H bonds include those that connect one side of strand 5 to strand 6 of the upper 50 kDa subdomain (which is linked to the C terminus of switch I), and the other side of strand 5 to strand 4 of the N-terminal subdomain. This maintenance of the connectivity between strands means that no rate-slowing breaking or reforming of these bonds need occur during the transitions between states.

Certain sequence features of helices HG and HH and loop 1 also facilitate the transducer's transitions between states. In contrast to the strands of the β sheet, helix HH and especially helix HG (which are connected to the N terminus of switch I) do undergo a shift between the rigor-like and non-rigor-like states: this displacement occurs both within the upper 50 kDa subdomain, relative to strands 6 and 7 (Figure 4A), and between this subdomain and helix HF of the N-terminal subdomain (Figure 4B). Moreover, numerous contacts are made between these elements in both states. Nevertheless, the shifting of these elements is facilitated by a repeat of 2 similarly sized apolar residues in helix HG that provide a "greasy patch" (Coureux et al., 2004) and appear to "substitute" for one another in the structure (Figure 4A). (Repeats of similar residues also promote "register slips" in other proteins [see Brown,

2006]). Loop 1 is the covalent link between helices HG of the upper 50 kDa subdomain and HF of the N-terminal subdomain (Figure 4B); thus, this element must necessarily change conformation as these helices shift relative to one another. Note, however, that in many isoforms, this loop is quite long and/or highly charged (see [Supplemental Data](#) available with this article online), and its structure, when seen, displays high crystallographic temperature factors. These features probably promote conformational variability that would lower the barrier to the transition between states.

Molluscan S1s, especially those from striated muscles, have unusually high basal ATPase rates compared to a variety of other myosins that show shortened and/or less charged loop 1s (see details in [Supplemental Data](#)). Moreover, certain isoforms exist longer in one state of the cycle than in another (Houdusse and Sweeney, 2001), which may also be accounted for by the structure of the transducer. For example, a complex salt bridge between helices HF and HG can be made only for the myosin V and myosin VI sequences, and only when these helices are arranged as in the rigor-like state (see Figure 4B). (This complex salt link is actually seen in the myosin VI structure [Mentrey et al., 2005].) A strong, stable actin-binding conformation is required for these isoforms' high duty ratio and efficient transport of cargo along F-actin. By contrast, another complex salt link—here between switch I and two N-terminal subdomain loops (Risal et al., 2004)—is observed only in the striated myosin II isoforms (of scallop, squid, and chicken), and only in the non-rigor-like position of switch I near the nucleotide (Figure 4B). Here, a low duty ratio is necessary for the rapid contraction of these myosins that form filaments.

It is important to clarify the energetics of the twisting/untwisting operation and its significance for the contractile cycle. In fact, as a rule, β sheets have a right-handed twist because that is its low-energy structure, and the untwisted state requires an input of energy (or the “straining” of bonds) (Wang et al., 1996). The twisting or coiling of the β sheet in the transducer has often been called a “distortion,” but it is the untwisted sheet that is, in fact, the distorted structure. In connection with our discussion below in the “Energetics” section, note that it is the untwisted transducer that characterizes the relatively rigid pre-power stroke, or primed, state, where ATP is present, and the fully twisted transducer that is present in the rigor-like state, which is nucleotide free. Hence, the untwisting of the β sheet helps to accommodate the higher-energy states that occur when ATP binds to myosin.

Additional Aspects of the Lever Arm

It is well known that the converter amplifies small motions of the other subdomains to produce large motions in the lever arm. Thus, the “recovery stroke” of the converter/lever arm module in the transition between rigor and post-rigor states (where it is “down”) to the pre-power stroke state (“up”) depends on the small movement of switch II toward the ATP-filled active site. This switch II movement “guides” the lower 50 kDa subdomain to close the inner part of the cleft, causing the converter to rotate about

two glycine pivots on either side of the SH1 helix (a part of the N-terminal subdomain) (Dominguez et al., 1998; Houdusse et al., 1999; Himmel et al., 2002; Fischer et al., 2005). The vicinity of the SH1 helix can be described as a “fulcrum” (“F” in Figure 5 inset) about which the converter and lever arm rotate (Uyeda et al., 1996). Not previously recognized to our knowledge, however, are changes in the interactions made by the converter and lever arm relatively far from the fulcrum in the various states of the motor.

The converter/lever arm module in the rigor-like state and in the post-rigor state, while similar, are structurally and functionally distinct (Figure 5). The rigor-like conformation of myosins II and V show well-conserved, close contacts between the C-terminal helix of the converter and loops that join the SH3 motif and the rest of the N-terminal subdomain. As noted above, in going from the rigor-like state to the post-rigor state, repositioning of switch I, by means of a partial untwisting of the transducer, causes a partial repositioning of switch II toward the nucleotide. In turn, the relay helix is slightly reoriented about a phenylalanine-rich region near its center (which is in close proximity to the SH1 helix), so that there is a small swing ($\sim 6^\circ$ – 20° in the various isoforms) of the converter/lever arm module. This movement partially breaks the contacts of the converter with the N-terminal subdomain. In this manner, the post-rigor structure portends their complete dissociation, which must precede formation of other weak actin-binding states.

The principal weak-binding state that defines the recovery stroke is the pre-power stroke state, visualized in progressively greater detail in the *Dictyostelium* (Fisher et al., 1995), chicken smooth (Dominguez et al., 1998), and *Argopecten irradians* (bay scallop) striated (Gourinath et al., 2003; Houdusse et al., 2000) isoforms. In this state, the positioning of switch II at the nucleotide site leads to a “kink” in the relay helix, just below the phenylalanine-rich region, which twists the lower relay loop (see Fischer, 1992 and Fischer et al., 2005). As a result, the converter and lever arm are now swung far away from the SH3 motif and toward the back of the N-terminal subdomain. Here, the C-terminal helix of the converter forms electrostatic interactions with positive charges on the N-terminal subdomain's HD/HE loop (as seen in the bay scallop [Gourinath et al., 2003] [Figure 5] and chicken smooth [Dominguez et al., 1998] structures). These contacts are among the farthest from the fulcrum in this state.

The other structurally characterized weak-binding state is the so-called internally uncoupled state (characterized by a disordered SH1 helix). Thus far, this state has been found only in bay scallop striated muscle (Himmel et al., 2002; Houdusse et al., 1999), but there is strong biochemical evidence for its presence in other myosin II isoforms (Burke and Reisler, 1977; Wells et al., 1980). Based on this structure's switch II position, transducer β sheet twist, and relay helix position/orientation, this state would appear to occur in the contractile cycle somewhere between the post-rigor and pre-power stroke states (also see Urbanke and Wray, 2001; Málnási-Csizmadia et al., 2001).

Note that in this state, unlike in the pre-power stroke state, the relay helix is “unkinked,” the lower relay loop is untwisted, and the converter and lever arm are now rotated toward the SH3 motif. Here, relatively far from the fulcrum, Arg96 of the ELC fills the major pocket in the center of this motif (Figure 5). Taken together, the contacts made by the converter/lever arm module described above provide additional stabilization for their respective states. Although noncovalent in nature, these contacts may be relatively difficult to break due to their locations far from the fulcrum.

Neither of these interactions between the converter/lever arm module and the N-terminal subdomain that are specific to weak actin-binding states can occur in myosin V. Here, the HD/HE loop has no positive charges, and there is no analogous pocket in the SH3 motif. These structural differences, together with those in the transducer and the 50 kDa cleft (five, altogether, as illustrated with asterisks in Figure 2A), would appear to extend the time spent by the myosin II isoforms in the weak binding states, relative to myosin V. Their effect could contribute to the very low duty ratio of myosin II, compared to that of myosin V. These findings suggest that the myosin lever arm plays a critical role in both step-size determination and kinetic tuning.

Anticipating the Strong Actin-Binding, Strong ADP-Binding Structure

The results that we have described on the nucleotide-free/rigor-like conformation provide some insights into possible structures of other strong actin-binding states that have been proposed, based on biochemical and physiological information. There is considerable evidence that one of these “missing structures” corresponds to a state in which a complex of myosin with MgADP is strongly bound to actin (Steffen and Sleep, 2004; Goldman, 1998; Spudich, 1994; Bagshaw and Trentham, 1974; Lynn and Taylor, 1971). At first sight, this state would seem to require a rigor-like closed cleft at the actin-binding surface, coexisting with a non-rigor-like switch I position near the nucleotide. In fact, fluorescence experiments suggest that the switch I loop and the actin-binding cleft do not move together as a rigid body, and that switch I has, in fact, two states in the presence of MgADP and a different one in the absence of nucleotide (Kintsjes et al., 2007). (The possibility has also been suggested, albeit without a specific model, that an as-yet unobserved transducer conformation may be responsible for producing the strong nucleotide-, strong actin-binding state [Coureux et al., 2004]).

A possible solution is suggested by the nucleotide-free structures of sea scallop myosin. As described above (Figure 3C), this isoform (striated or catch) shows a closed outer cleft, but an incompletely closed inner cleft with switch I, but not switch II, repositioned part-way toward the nucleotide-binding site. As a consequence, the electrostatic attraction between Arg247 of switch I and Glu468 of switch II (squid numbering; see Figure 3A) appears to be weakened in the sea scallop isoform. This finding supports a previous proposal (Himmel et al., 2002) that it is the breaking of this salt bridge and nearby hydrogen bonds, between switches I and II, that actually triggers

the power stroke. This structure thus displays “incomplete” communication between the actin-binding and nucleotide-binding regions, compared to the squid myosin structure. Examination of all of the myosin isoform structures available (including myosin V) reveals that an insertion/interruption between helices HQ and HR (in the lower 50 kDa subdomain, Figure 3C) is present, albeit with isoform-specific lengths and composition. We would expect that such a loop structure might impart flexibility between different states of the same isoform in the same way it is seen to impart conformational differences between the sea scallop and the squid nucleotide-free structures. The sea scallop nucleotide-free structures may thus presage conformational features that are necessary for the strong actin-binding, strong ADP-binding state of myosin.

Coda

Here, we describe some key implications of our findings.

Allostery and Transduction Pathways in Myosin

During the past decade, our views on allostery have greatly evolved. Large, multidomain enzymes (and motors), such as myosin, have been analyzed, both experimentally and by computational methods, to establish how distant sites communicate with one another. For example, use of the “conjugate peak refinement” method (Fischer, 1992; Fischer et al., 2005) has recently allowed for the generation of a detailed structural model for the so-called recovery stroke in myosin. Their results yield a straightforward, mechanistic description of the coupling between the nucleotide-binding site (switch II) and the converter/lever arm module between the post-rigor and pre-power stroke states (in the forward direction called the recovery stroke). The current crystal structures of the rigor-like state that we have described are especially informative about these pathways.

One finding that we have reported is the small but reproducible difference in the position of the converter/lever arm module between the rigor-like and post-rigor states. This difference is also coupled to a relatively small difference in the position of switch II. The functional importance of this difference is that there are certain rigor-like-specific interactions between the converter and the N-terminal subdomain, including some that are conserved in all of the myosin II and myosin V rigor-like structures, that must be broken to allow the converter/lever arm module to swing to the pre-power stroke state position during the recovery stroke. The rigor-like to post-rigor transition begins the process of breaking these bonds. In this sense, the rigor-like state may, in fact, be considered the real starting point of the recovery stroke, with the pre-power stroke state remaining as the end point. In contrast to work by Fischer et al. (2005), who begin their simulations with a post-rigor structure, the post-rigor state (and, in some cases, the internally uncoupled state) may be thought of as an “intermediate” in the recovery stroke (albeit much closer to the starting point than to the end point).

The second related point is the importance of interactions between the converter/lever arm module and the N-terminal subdomain in various weak actin-binding states,

as well as in the rigor-like state. Fischer et al. (2005) mention that the coupling between the nucleotide and lever arm “can work either way,” i.e., lever arm \rightarrow ATP, as well as ATP \rightarrow lever arm; however, the driving force for the mechanism is described only in the conventional forward manner (ATP \rightarrow lever arm), where changes in the nucleotide site cause changes in the position in an otherwise “passive” converter/lever arm. The interactions between the converter/lever arm module and the N-terminal subdomain might, in fact, promote the reverse pathway, i.e., converter/lever arm to nucleotide site as well as converter/lever arm to actin-binding site. Note that the interactions between the converter/lever arm module and the N-terminal subdomain that are seen in the myosin II internally uncoupled and pre-power stroke state structures (two of the red asterisks in Figure 2A) may not form as strongly—or, indeed, at all—in myosin V, in which the residues involved in these interactions are different. In this way, the converter/lever arm module can actively promote relatively strong nucleotide-binding and relatively weak actin-binding conformations in the myosin IIs.

A Few Comments on Energetics

The current results also have implications for the mechanical roles of the parts of the motor in the contractile cycle. Holmes and coworkers have suggested that the power stroke occurs primarily to relieve molecular strain from a kink in the relay helix that is seen in the pre-power stroke conformation. Thus, the twisting of the seven-stranded β sheet is a way to relieve this kink, leading to the swinging of the lever arm in the power stroke (Geeves and Holmes, 2005). In our view, molecular strain in a number of structural elements of the pre-power stroke conformation, including the untwisted β sheet and the kinked relay helix, stores the energy from the binding and hydrolysis of ATP. Evidence has been presented that strong actin binding is a major contributor to the loss of free energy needed to perform work during the power stroke (Karatzafieri et al., 2004). It is also possible, however, that the transducer twist has a role in the energetics (for example, by abolishing certain interactions between switches I and II). The power stroke repositions the lower 50 kDa subdomain and the converter, directing the lever arm to a rigor-like orientation (Houdusse et al., 1999; Himmel et al., 2002); sliding of strands of the seven-stranded β sheet may further facilitate this motion (Coureux et al., 2003). The various structures of the myosin head in the rigor-like conformation, analyzed here, indicate that the kink in the relay helix is abolished and that the seven-stranded β sheet relaxes to the twisted conformation immediately after the power stroke (Coureux et al., 2004; Reubold et al., 2003). However, the exact pathway utilized for release of inorganic phosphate remains uncertain.

Since the energy state of the myosin head increases as the transducer untwists, a new understanding of the actomyosin cycle begins to emerge that may support a thermodynamic role for the internally uncoupled state. As mentioned above, the transducer untwists incrementally as myosin changes conformation from rigor-like to post-rigor to internally uncoupled to pre-power stroke, supporting

the view that the ATP-bound conformations are in a higher-energy state than the nucleotide-free/rigor-like conformation. The highest-energy state is reached in the pre-power stroke conformation, just before ATP hydrolysis, and it is possible that a thermodynamic barrier exists between the post-rigor and pre-power stroke conformations, in the form of the energy of activation that must be overcome in changing between these two conformations. The internally uncoupled state, by temporarily disengaging the mechanical elements of the myosin motor, may lower this barrier and make the transition between post-rigor and pre-power stroke a thermodynamically reversible process (also see Urbanke and Wray, 2001; Málnási-Csizmadia et al., 2001). With the gear work of the molecular motor disengaged (by the melting of the SH1 helix), most of the remaining molecular strain would be attributable to the untwisting of the transducer. Even the kink in the relay helix would not form until the SH1 helix reforms in the pre-power stroke conformation. If this is so, then this conformational transition would be more rapid if it passes through the internally uncoupled state than if it does not. Thus, it is possible that the internally uncoupled state provides a thermodynamic pathway that lowers the energy barrier between the post-rigor and pre-power stroke states by limiting the energetic cost to the further untwisting of the transducer. The view that the internally uncoupled state is an *in vivo* rather than off-pathway *in vitro* state is supported by previous biochemical (Reisler et al., 1974; Wells et al., 1980) and structural data (Himmel et al., 2002; Gourinath et al., 2003).

EXPERIMENTAL PROCEDURES

Sea scallops and squid were obtained from the Marine Biological Laboratory (MBL) in Woods Hole, Massachusetts. Striated and catch muscles were harvested from scallop, and the funnel retractor muscle was harvested from squid. Scallop striated and squid muscle myosin were prepared as described (Stafford et al., 1979), with slight modifications for scallop catch muscle; S1 was prepared as described (Kalabokis and Szent-Györgyi, 1997), with modifications. S1 crystals were obtained by using the hanging-drop vapor-diffusion technique at 4°C. The final crystals were flash frozen in liquid nitrogen prior to data collection. X-ray diffraction data were collected at the Cornell High Energy Synchrotron Source (CHESS), beamline A1. The rigor-like crystal structures of S1 without bound nucleotide have been determined to a resolution of 3.25 Å for sea scallop catch and striated muscles and to 2.6 Å for squid. Post-rigor crystal structures of S1 from squid and sea scallop catch muscle bound to ADP were determined to 3.1 Å. Details of procedures and a table of crystallographic statistics are included in Supplemental Data.

Supplemental Data

Supplemental Data include a detailed Experimental Procedures section, a table of crystallographic statistics, a table of loop 1 properties, and detailed figure legends and are available at <http://www.structure.org/cgi/content/full/15/5/553/DC1/>.

ACKNOWLEDGMENTS

This work was supported by the following grants: to C.C. from the National Institute of Arthritis and Musculoskeletal and Skin Diseases of the National Institutes of Health (NIH) (AR017346); to M.K. from the NIH (Research Grant #D43 TW006230 [1 R01 TW007241-01] funded by the Fogarty International Center and the National Heart, Lung,

and Blood Institute), a European Molecular Biology Organization-Howard Hughes Medical Institute Startup Grant for Central Europe, and the Bolyai Fellowship of the Hungarian Academy of Sciences; to L.N. by Hungarian Scientific Research Fund (OTKA) grants K61784 and TS049812; and to D.M.H. by an NIH National Research Service Award fellowship (F32 AI 060300). We thank E. Enos at the Marine Biological Laboratory, Woods Hole, MA, for assistance with obtaining squid, Z. Zhou for related crystallographic work, the staff at the Cornell High Energy Synchrotron Source for assistance with data collection, A. Houdusse for critical reading of the manuscript, and L. Lynch for manuscript preparation.

Received: December 12, 2006

Revised: March 11, 2007

Accepted: March 14, 2007

Published: May 15, 2007

REFERENCES

- Atkins, P. (1990). *Physical Chemistry*, Fourth Edition, Section 28.2 (Oxford, UK: Oxford University Press).
- Bagshaw, C.R., and Trentham, D.R. (1974). The characterization of myosin-product complexes and of product-release steps during the magnesium ion-dependent adenosine triphosphatase reaction. *Biochem. J.* **141**, 331–349.
- Brown, J.H. (2006). Breaking symmetry in protein dimers: designs and functions. *Protein Sci.* **15**, 1–13.
- Burke, M., and Reisler, E. (1977). Effect of nucleotide binding on the proximity of the essential sulfhydryl groups of myosin. Chemical probing of movement of residues during conformational transitions. *Biochemistry* **16**, 5559–5563.
- Coureux, P.D., Wells, A.L., Menetrey, J., Yengo, C.M., Morris, C.A., Sweeney, H.L., and Houdusse, A. (2003). A structural state of the myosin V motor without bound nucleotide. *Nature* **425**, 419–423.
- Coureux, P.D., Sweeney, H.L., and Houdusse, A. (2004). Three myosin V structures delineate essential features of chemo-mechanical transduction. *EMBO J.* **23**, 4527–4537.
- De La Cruz, E.M., Wells, A.L., Rosenfeld, S.S., Ostap, E.M., and Sweeney, H.L. (1999). The kinetic mechanism of myosin V. *Proc. Natl. Acad. Sci. USA* **96**, 13726–13731.
- Dominguez, R., Freyzon, Y., Trybus, K.M., and Cohen, C. (1998). Crystal structure of a vertebrate smooth muscle myosin motor domain and its complex with the essential light chain: visualization of the pre-power stroke state. *Cell* **94**, 559–571.
- Fischer, S., Windshugel, B., Horak, D., Holmes, K.C., and Smith, J.C. (2005). Structural mechanism of the recovery stroke in the myosin molecular motor. *Proc. Natl. Acad. Sci. USA* **102**, 6873–6878.
- Fischer, S.K.M. (1992). Conjugate peak refinement - an algorithm for finding reaction paths and accurate transition -states in systems with many degrees of freedom. *Chem. Phys. Lett.* **194**, 252–261.
- Fisher, A.J., Smith, C.A., Thoden, J., Smith, R., Sutoh, K., Holden, H.M., and Rayment, I. (1995). Structural studies of myosin:nucleotide complexes: a revised model for the molecular basis of muscle contraction. *Biophys. J.* **68**, 19S–26S.
- Fujita-Becker, S., Reubold, T.F., and Holmes, K.C. (2006). The actin-binding cleft: functional characterisation of myosin II with a strut mutation. *J. Muscle Res. Cell Motil.* **27**, 115–123.
- Geeves, M.A., and Holmes, K.C. (2005). The molecular mechanism of muscle contraction. *Adv. Protein Chem.* **71**, 161–193.
- Goldman, Y.E. (1998). Wag the tail: structural dynamics of actomyosin. *Cell* **93**, 1–4.
- Gourinath, S., Himmel, D.M., Brown, J.H., Reshetnikova, L., Szent-Györgyi, A.G., and Cohen, C. (2003). Crystal structure of scallop myosin S1 in the pre-power stroke state to 2.6 Å resolution: flexibility and function in the head. *Structure* **11**, 1621–1627.
- Himmel, D.M., Gourinath, S., Reshetnikova, L., Shen, Y., Szent-Györgyi, A.G., and Cohen, C. (2002). Crystallographic findings on the internally-uncoupled and near-rigor states of myosin: further insights into the mechanics of the motor. *Proc. Natl. Acad. Sci. USA* **99**, 12645–12650.
- Holmes, K.C., Schroder, R.R., Sweeney, H.L., and Houdusse, A. (2004). The structure of the rigor complex and its implications for the power stroke. *Philos. Trans. R. Soc. Lond. B Biol. Sci.* **359**, 1819–1828.
- Houdusse, A., and Cohen, C. (1996). Structure of the regulatory domain of scallop myosin at 2 Å resolution: implications for regulation. *Structure* **4**, 21–32.
- Houdusse, A., and Sweeney, H.L. (2001). Myosin motors: missing structures and hidden springs. *Curr. Opin. Struct. Biol.* **11**, 182–194.
- Houdusse, A., Kalabokis, V.N., Himmel, D., Szent-Györgyi, A.G., and Cohen, C. (1999). Atomic structure of scallop myosin subfragment S1 complexed with MgADP: a novel conformation of the myosin head. *Cell* **97**, 459–470.
- Houdusse, A., Szent-Györgyi, A.G., and Cohen, C. (2000). Three conformational states of scallop S1. *Proc. Natl. Acad. Sci. USA* **97**, 11238–11243.
- Kalabokis, V.N., and Szent-Györgyi, A.G. (1997). Cooperativity and regulation of scallop myosin and myosin fragments. *Biochemistry* **36**, 15834–15840.
- Karatzafieri, C., Chinn, M.K., and Cooke, R. (2004). The force exerted by a muscle cross-bridge depends directly on the strength of the actomyosin bond. *Biophys. J.* **87**, 2532–2544.
- Kintses, B., Gyimesi, M., Pearson, D.S., Geeves, M.A., Zeng, W., Bagshaw, C.R., and Málnási-Csizmadia, A. (2007). Reversible movement of switch 1 loop of myosin determines actin interaction. *EMBO J.* **26**, 265–274.
- Lymn, R.W., and Taylor, E.W. (1971). Mechanism of adenosine triphosphate hydrolysis by actomyosin. *Biochemistry* **10**, 4617–4624.
- Málnási-Csizmadia, A., Pearson, D.S., Kovács, M., Woolley, R.J., Geeves, M.A., and Bagshaw, C.R. (2001). Kinetic resolution of a conformational transition and the ATP hydrolysis step using relaxation methods with a *Dictyostelium* myosin II mutant containing a single tryptophan residue. *Biochemistry* **40**, 12727–12737.
- Menetrey, J., Bahloul, A., Wells, A.L., Yengo, C.M., Morris, C.A., Sweeney, H.L., and Houdusse, A. (2005). The structure of the myosin VI motor reveals the mechanism of directionality reversal. *Nature* **435**, 779–785.
- Rayment, I., Holden, H.M., Whittaker, M., Yohn, C.B., Lorenz, M., Holmes, K.C., and Milligan, R.A. (1993a). Structure of the actin-myosin complex and its implications for muscle contraction. *Science* **261**, 58–65.
- Rayment, I., Rypniewski, W.R., Schmidt-Bäse, K., Smith, R., Tomchick, D.R., Benning, M.M., Winkelmann, D.A., Wesenberg, G., and Holden, H.M. (1993b). Three-dimensional structure of myosin subfragment-1: a molecular motor. *Science* **261**, 50–58.
- Reisler, E., Burke, M., Himmelfarb, S., and Harrington, W.F. (1974). Spatial proximity of the two essential sulfhydryl groups of myosin. *Biochemistry* **13**, 3837–3840.
- Reubold, T.F., Eschenburg, S., Becker, A., Kull, F.J., and Manstein, D.J. (2003). A structural model for actin-induced nucleotide release in myosin. *Nat. Struct. Biol.* **10**, 773–775.
- Risal, D., Gourinath, S., Himmel, D.M., Szent-Györgyi, A.G., and Cohen, C. (2004). Myosin S1 structures reveal a novel nucleotide conformation and a complex salt bridge that helps couple nucleotide and actin binding. *Proc. Natl. Acad. Sci. USA* **101**, 8930–8935.
- Spudich, J.A. (1994). How molecular motors work. *Nature* **372**, 515–518.
- Stafford, W.F., 3rd, Szentkiralyi, E.M., and Szent-Györgyi, A.G. (1979). Regulatory properties of single-headed fragments of scallop myosin. *Biochemistry* **18**, 5273–5280.

Steffen, W., and Sleep, J. (2004). Using optical tweezers to relate the chemical and mechanical cross-bridge cycles. *Philos. Trans. R. Soc. Lond. B Biol. Sci.* 359, 1857–1865.

Sweeney, H.L., and Houdusse, A. (2004). The motor mechanism of myosin V: insights for muscle contraction. *Philos. Trans. R. Soc. Lond. B Biol. Sci.* 359, 1829–1841.

Urbanke, C., and Wray, J. (2001). A fluorescence temperature-jump study of conformational transitions in myosin subfragment 1. *Biochem. J.* 358, 165–173.

Uyeda, T.Q., Abramson, P.D., and Spudich, J.A. (1996). The neck region of the myosin motor domain acts as a lever arm to generate movement. *Proc. Natl. Acad. Sci. USA* 93, 4459–4464.

Wang, L., O'Connell, T., Tropsha, A., and Hermans, J. (1996). Molecular simulations of β -sheet twisting. *J. Mol. Biol.* 262, 283–293.

Wells, J.A., Knoeber, C., Sheldon, M.C., Werber, M.M., and Yount, R.G. (1980). Cross-linking of myosin subfragment 1. Nucleotide-enhanced modification by a variety of bifunctional reagents. *J. Biol. Chem.* 255, 11135–11140.

Accession Numbers

Coordinates have been deposited in the Protein Data Bank with accession codes 2OVK, 2OS8, 2OY6, and 2OTG. Please see additional information about deposited coordinates in [Table S1](#).